Proceedings of 10th International Conference on Precision, Meso, Micro and Nano Engineering (COPEN 10)
December 07 – 09, 2017, Indian Institute of Technology Madras, Chennai – 600 036 INDIA

Influence of Tool Geometry on Residual Stresses in Vibration Assisted Turning of Ti6Al4V Alloy

D Venkata Sivareddy*, P Vamsi Krishna, A Venu Gopal

Department of Mechanical Engineering, National Institute of Technology, Warangal-506004, INDIA

Abstract

Vibration Assisted Turning (VAT) is an effective machining process for hard materials like Ti6Al4V alloy to control surface integrity of machined components. Residual stresses induced during machining of Ti6Al4V alloy have detrimental effect on surface quality of the machined components. The cutting tool geometry parameters such as rake angle and nose radius have significant impact on residual stress distribution along the depth of machined surface. The residual stress under different cutting conditions in VAT of Ti alloy is analyzed by FEM simulation. It is observed that the circumferential residual stresses (CRS) changes its nature from tensile to compressive at certain depth from machined surface. The compressive CRS layer thickness is increased whereas compressive Axial Residual Stress (ARS) layer thickness is decreased with increase in rake angle in VAT process. The compressive layer thickness of CRS and ARS is decreased with increase in nose radius.

Keywords: Vibration Assisted Turning, FEM, Residual Stress, Rake Angle, Nose Radius

1. INTRODUCTION

Ti6Al4V alloy is the most commonly used in aerospace and automobile applications. Machining of Ti6Al4V is difficult due to high machining temperatures, which are sufficiently high enough to thermally soften the tool and cause rapid tool wear. This results in poor surface finish and enhanced cutting forces, which leads to hampering machinability. Vibration Assisted Turning (VAT) exhibited promising results [1-2] in machining high strength materials due to intermittent contact with the workpiece at periodic intervals. This aids in enhancement of tool life, reduction in cutting temperature, improvement in surface finish and reduction in production cost by reducing the time of contact [6].

Residual stresses developed in machining are a major problem in machining of titanium alloys. Generation of residual stresses depends on thermoplastic deformation of the workpiece. They may develop due to plastic deformation of material or volume changes that occur due to thermo-mechanical loads. Mechanical loads induce plastic deformation by displacing the crystal structure, which in turn generates thermal loads. Further the friction at tool chip interface acts as the main source for thermal load, which causes volume changes due to thermal gradient. However, the stresses due to mechanical loading are predominant [3]. The residual stresses developed will extend from surface of cut to certain depth due to thermo-mechanical loads and gradually diminish as the depth increases. Surface residual stresses affect the fatigue life and tribological properties of a machined surface, hence the product life. Based on the nature and magnitude of stress state they can be either beneficial or detrimental [4]. The nature of residual stress depends on cutting conditions, work material, cutting tool geometry and contact conditions. Residual stresses are predominantly tensile due to thermal loads and pertain near surface, whereas compressive residual stress developsalong the depth of machined surfacedue to mechanical load. Friction plays an important role in case of tensile residual stress as it generates high temperatures and eventually thermal loads at surface. The machined surface cools at faster rate compared to subsurface, hence the surface contracts and is subjected to compressive loading. When the strains drop to zero, the resulting residual stress will be tensile in nature. The opposite occurs in subsurface hence the resultant stresses are compressive residual stress. The evidence of residual stress finally diminishes as we move away from the surface [5]. Hence the fundamental mechanism and nature of residual stresses that develop due to VAT should be analyzed, to enhance the performance.

Based on literature, most of the investigations are related to evaluating the performance of VAT in relation to the cutting forces, cutting temperature by simulation or experimentation [6-7]. A limited research was observed towards the analysis of residual stresses developed in workpiece due to VAT. The objective of this study is to investigate the effect of rake angle and tool nose radius in residual stress distribution on machined component in VAT of Ti6Al4V. A Finite element model (FEM) is developed in ABAQUS frame work and validated with the literature [8]. The 3-D FE orthogonal machining model is used to study the residual stresses in the machined surface and their variation in each stage of VAT.

2. FINITE ELEMENT MODELING OF VAT PROCESS

2.1. Finite element simulation of VAT

A 3D FE model for orthogonal machining is developed in ABAQUS and Dynamic explicit temperature Displacement solver is used in this simulation. The workpiece material Ti6Al4V is modeled by considering it as isotropic plastic material subjected to strain rate of 2000 s^{-1}. Tungsten carbide (WC) cutting tool is assumed as rigid to reduce the simulation time. The ultrasonic vibration with a frequency of 20 kHz and amplitude of 20 µm is imposed on movement of cutting tool. The details of tool, workpiece and machining conditions used in this simulation are listed in table 1. The type of mesh element used in this simulation is coupled temperature- displacement type to facilitate both mechanical and thermal loading. This model consists of approximately 5400 elements for workpiece. Figure 1 shows the relative movement between tool and workpiece in simulation. In this model, workpiece moves with a constant velocity Vc that equals to 30 m/min. The kinematic boundary conditions for all sides of workpiece are Vx= Vc and Vy=0.The cutting tool is considered as rigid and it is immovable for conventional turning (CT).and tool vibrates in cutting velocity direction in VAT as shown in Fig 1. The

ISBN: 978-93-80689-28-9

condition for separation of tool from workpiece during VAT is cutting tip vibrating velocity V of the tool must be greater than linear velocity of the workpiece or too(Vc).For frequency f=20 kHz and amplitude a= 20 µm ,u_x= -a cosωt, u_y=0 where ω= 2πf is angular velocity of the tool. The cutting tip vibration velocity V = a ω sin ωt, and a ω=2512>Vc (30 m/min).

Table 1: FE Modeling parameters used in the simulation

Materials	Workpiece: Ti6Al4V Cutting tool:Tungsten carbide
Machining Conditions for simulation	Speed : 30 m/min Width of cut : 0.2 mm Coefficient of friction(µ)=0.6 Element:C3D8RT Element shape: Hex dominated Element type : Coupled temperature displacement type Meshing:ALE adaptive mesh with frequency of 100 Remeshing sweeps per increment:1 Interaction : General contact Interface friction : General behaviour, Penalty contact

2.2 Johnson-Cook Material model

The Jonson cook constitutive material model considers the plastic flow stress as a function of strain hardening, strain rate and thermal softening. The JC material model is given by an equation (1) [9].

$$\sigma_{eq} = [A + B(\varepsilon)^n]\left[1 + C \times ln\left(\frac{\varepsilon^o}{\varepsilon_0^o}\right)\right][1 - (\frac{T - T_{room}}{T_{Melt} - T_{room}})^m] \quad (1)$$

Where σ_{eq} is the equivalent stress, ε is equivalent plastic strain; $\varepsilon^{\circ}/\varepsilon^{o}_0$ is the reference strain rate. T_{Melt} is the melting temperature; T_o is transition temperature defined as room temperature of 27°C.A, B, C, n and m are material constants. Where, A is initial yield stress, B is hardening modulus, C is strain rate dependent coefficient, n is work hardening exponent, m is the thermal softening coefficient.

2.3 Separation criteria and Damage equation

The chip separation behavior and the chip crack initiation or growth, which is based on the value of the equivalent plastic strain at element integration points. According to JC model damage parameter D is given by:

$$D = \sum\left(\frac{\Delta\epsilon_p}{\epsilon_f}\right) \quad (2)$$

Where $\Delta\epsilon_p$ is increment of the equivalent plastic strain which is updated at every analysis increment; ϵ_f is equivalent strain at failure and is expressed as

$$\epsilon_f = \left[D_1 + D_2\, exp\left(D_3 \frac{p}{q}\right)\right]\left[1 + D_4\, ln\left(\frac{\epsilon_P}{\epsilon}\right)\right][1 + D_5 T^*] \quad (3)$$

Where $\Delta\epsilon_p$ depends on non-dimensional equivalent plastic strain rate and $\Delta\epsilon_p / \epsilon_f$, the ratio of hydrostatic pressure to Von-Mises equivalent stress is p/q, (d1~ d5) are the damage constants, T* is the homologous to the JC model equation.

3. RESULTS AND DISCUSSION

The objective of this work is to analyzethe influence of tool geometry (rake angle and nose radius) on residual stress distribution in VAT of Ti6Al4V alloy at different depths of cut. The residual stresses developed on machined surfaces are evaluated in circumferential and axial directions at a depth ranging from 0 to 100µm. The residual stresses are evaluated taking the average value at three sections on machined surface as shown in fig 2.

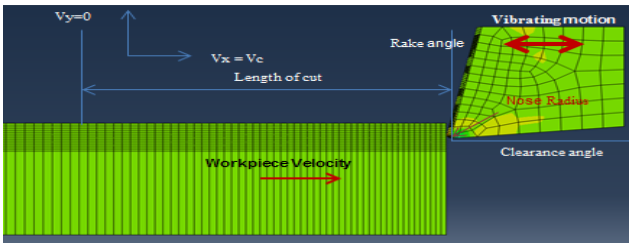

Fig 1.FE Modeling of orthogonal VAT process

Table 2 Material Model and JC model parameters used in simulation

Density			4420 kg/m3			
Conductivity			7.264w/m-K			
Young's modulus			114 GPa			
Inelastic heat fraction			0.9			
Specific heat			526 kJ/kg-K			
JC- Parameters						
A MPa	B MPa	C	n	m	Melting temperature ˚C	Strain Rate s^{-1}
724.7	683.1	0.035	0.47	1	1650	2000
Damage parameters						
d1		d2	d3		d4	d5
-0.09		0.28	0.48		0.014	3.18

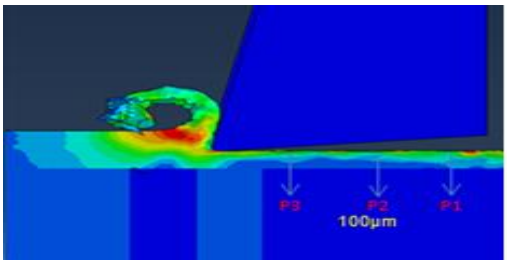

Fig 2.Residual stress measurement technique in simulation

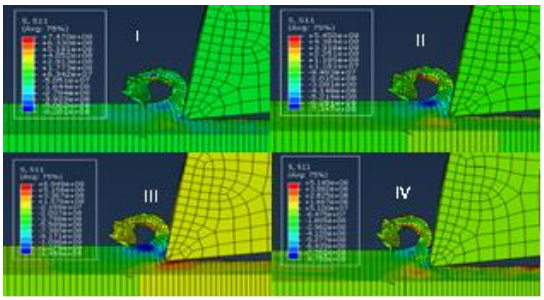

Fig 3. Development of CRS in four stages of one cycle of vibration

The residual stresses are transient and vary with stages involved in harmonic motion of VAT due to dynamic variation of forces. Figure 3 shows various stages of vibration cycle during VAT. During I stage, tool approaches the chip where CRS varies from 747 MPa tensile to 620MPa compressive. In II stage, the tool comes in contact with chip where CRS varies from 545 MPa tensile to 734 MPa compressive. In III stage, tool penetrates into chip where CRS varies from 694 MPa tensile to 1429 MPa compressive. The maximum tensile stress state is observed in this stage due to initiation of deformation. These stress states

are observed in primary and secondary deformation zones. In IV stage, the tool unloaded from chip, where CRS varies from 514 MPa tensile to 875 MPa compressive. In every stage, the magnitude of tensile and compressive residual stresses is due to thermal and mechanical loads respectively.

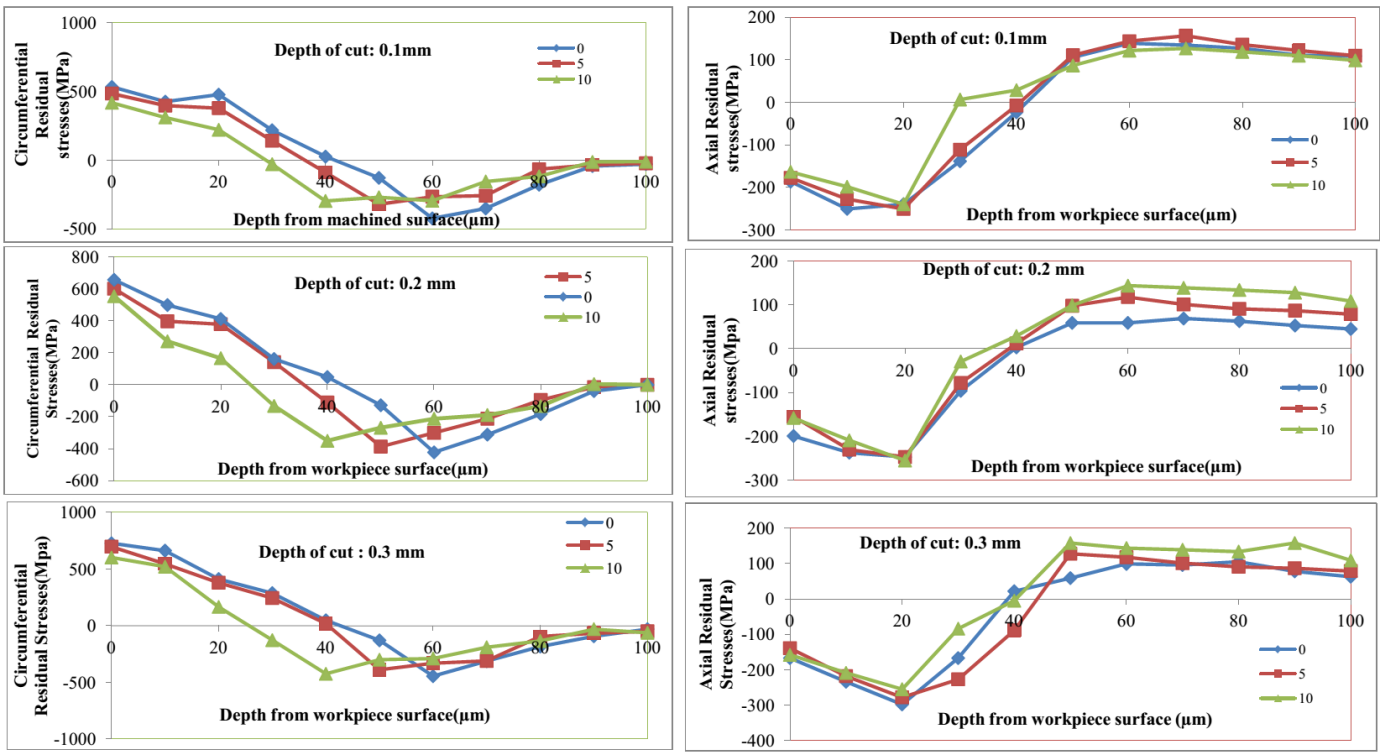

Fig 4: CRS and ARS distribution along depth of machined surface for various rake angles at different depths of cut

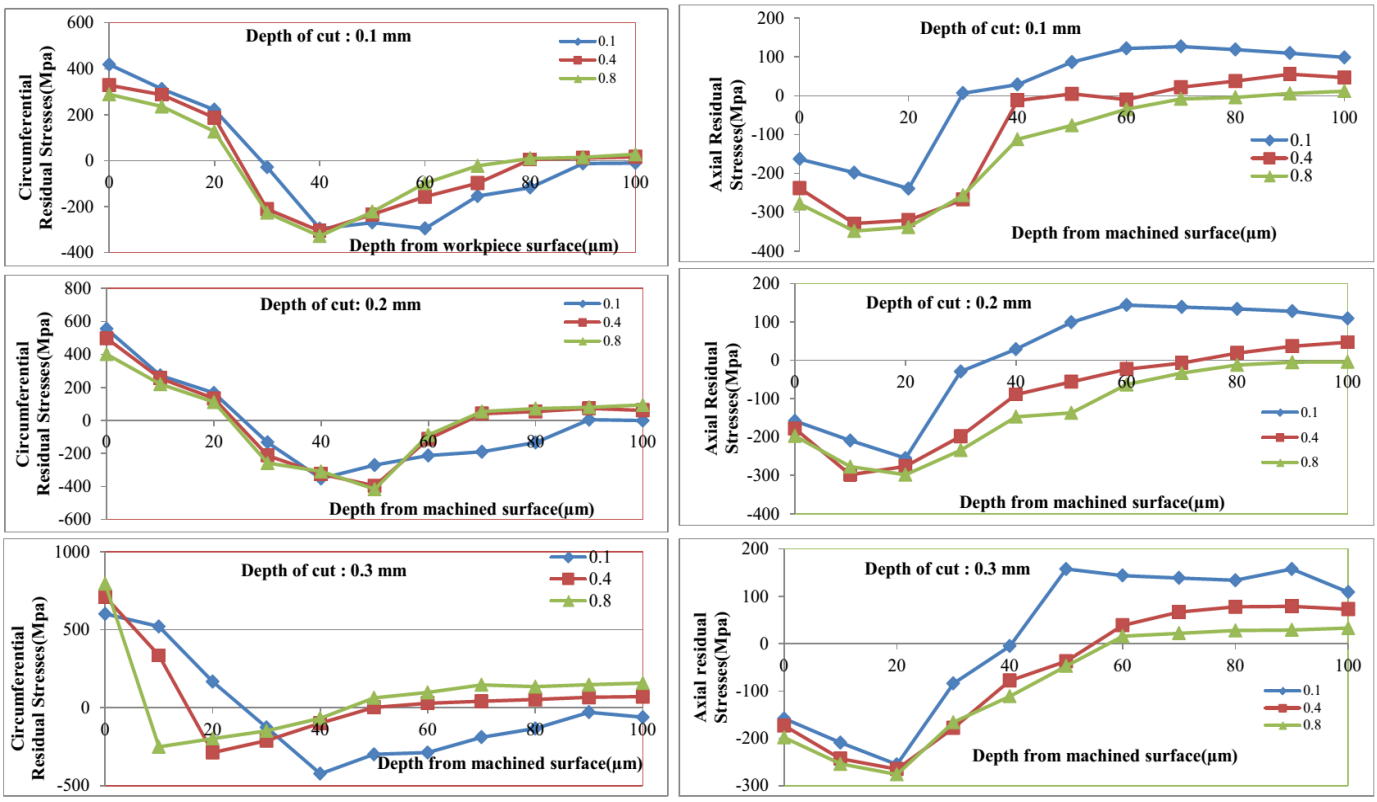

Fig 5: CRS and ARS distribution along depth of machined surface for various nose radius at different depth of cuts

3.1 Effect of rake angle on residual stresses

The cutting edge geometry has more impact on stress levels generated in machining process. The CRS generated in machined surface are tensile in nature with different rake angle. However, these stresses change its nature from tensile to compressive at certain depth beneath the surface. The maximum compressive stresses and effected depth are analyzed with change in rake angle of tool in this study. The CRS and ARS are evaluated for 0^o, 5^o and 10^o rake angles at various depths of cut. Figure 4. Shows CRS and ARS depth profiles for various rake angles at different depths of cut. The maximum compressive CRS is 534MPa at a depth of 60µm and the depth when the residual stresses changes from tensile to compressive is about 40µm for 0^o rake angle at 0.1mm depth of cut. The maximum compressive CRS and effected depth is reduced with increase in rake angle. The CRS are also evaluated at 0.2 mm and 0.3 mm depth of cuts. The tensile CRS at surface are increased with increase in depth of cut. But the maximum compressive CRS and effected depth are not much varied with depth of cut. Similarly, ARS also evaluated for different rake angles at different depths of cut. The nature of ARS at surface is compressive and its changes nature from compressive to tensile at certain depth from machined surface [5]. The maximum compressive ARS is 239 MPa at a depth of 20µm and this compressive nature exists upto 40 µm depth. After that the nature of ARS is tensile and remains same upto 100 µmat 0.1mm depth of cut. The ARS are also evaluated at 0.2mm and 0.3 mm. The magnitude of compressive ARS at surface is reduced with increase in depth of cut. But the maximum ARS and nature of ARS along depth are not much effected with increase in depth of cut.

3.2. Effect of nose radius on residual stresses

Figure 5 shows the results of CRS and ARS for 0.4 µm and 0.8 µm nose radius at 0.1 mm, 0.2 mm and 0.3 mm depths of cut. The compressive CRS and ARS exist at the machined surface for both nose radii. The compressive residual stress at machined surface and maximum residual stress induced beneath the surface are different greatly. For nose radius 0.4 µm, compressive CRS at machined surface is 239 MPa and it increases to a maximum of 327 MPa at a depth of 20µm .Then compressive CRS decreases with increase in depth and changes its nature in to tensile at a depth of 60 µm and maintains constant for remaining depth. For 0.8µm nose radius, the magnitude of CRS at surface is less in comparison with 0.4 µm nose radius, but same trend is observed throughout the depth of the machined surface. The magnitude of maximum compressive and tensile CRS is more in comparison with 0.4 µm nose radius. The magnitude of compressive CRS induced at the surface is decreased with increase in depth of cut. In case of ARS, compressive residual stresses are induced throughout the depth. The maximum compressive ARS is less in comparison with CRS for all depth of cuts. The depth at which maximum compressive ARS observed is different from CRS.

4. CONCLUSIONS

The following conclusions are drawn from this study.

Moderate compressive residual stresses are generated in first two stages of VAT. The maximum compressive residual stresses are generated in III stage of VAT due to dynamic variation of mechanical and thermal loads.

The compressive layer thickness of CRS increased and ARS decreased with an increase in rake angle in machined surface in VAT process. The maximum compressive CRS and ARS are not much effected with rake angle and depth of cut.

The tool nose radius affects the residual stress at the machined surface significantly at early cutting stage. The compressive layer thickens in machined component is decreased with increase in nose radius. The maximum compressive CRS and ARS are decreased and increased respectively with increase in nose radius.

References

[1] D.E. Brehl, T.A. Dow, Review of vibration-assisted machining, Precision Engineering, Vol. 32, 153–172, 2008.

[2] R. C. Skelton, Effect of ultrasonic vibration on the turning process, International Journal of Machine Tool Design and Research Vol. 9, 363 374, 1969.

[3] Y. B. Guo, C. R. Liu, 3D FEA Modeling of hard turning, Journal of Manufacturing Science and Engineering, Vol. 124, 189-198 2002,.

[4]J.C. Outeiroa, J.P. Costesa, J.R. Kornmeierb, Cyclic variation of residual stress induced by tool vibration in machining operations, ProcediaCIRP,Vol. 8,493–497,2013.

[5] Jeffrey D. Thiele, Shreyes N. Melkote, Effect of cutting-edge geometry and workpiece hardness on surface residual stresses in finish hard turning of AISI 52100 steel, Journal of Manufacturing Science and Engineering, Vol.122, 642-649, 2000.

[6] Chandra Nath, M. Rahman, S. S. K. Andrew, A study on ultrasonic vibration cutting of low alloy steel, Journal of Materials Processing Technology, Vol. 192–193,159–165,2007.

[7] N. Ahmed, A.V. Mitrofanov, V.I. Babitsky, V.V. Silberschmidt, Analysis of forces in ultrasonically assisted turning, Journal of Sound and Vibration, Vol. 308,845–854,2007.

[8] Patil, S., Joshi, S., Tewari, A. and Joshi, S.S. 'Modeling and simulation of effect of ultrasonic vibrations on machining of Ti-6Al-4V', Ultrasonic, Vol. 54,694–705,2014.

[9] Johnson G. R. and Cook W. H., A constitutive model and data for metals subjected to large strains, high strain rates, and high temperatures. Proceedings, 7th International Symposium on Ballistics, Hague, Netherlands, April 1983.